Granular Matter manuscript No.
(will be inserted by the editor)

Eigenparticles: Characterizing particles using Eigenfaces

J.E. Higham · A. Vaidheeswaran · K. Benavides Meneses · P. Shepley

Received: date / Accepted: date

Abstract The shape characteristics of particles have a pinnacle role in microsopic and macroscopic features of a system. Several studies have highlighted the need for considering deviations from a spherical representation of particles for accurate modeling of granular and multiphase flow systems. Using a shape factor, sphericity or roundness parameter alone is proven to be inadequate to capture the physical phenomena. In the present study we propose a novel metric based on the pattern recognition method Eigenfaces, coining the technique 'Eigenparticles'. Using this technique we create a single statistical distribution of basis shapes to describe the morphological composition. The proposed technique is successfully validated with test shapes and applied to real particles. When compared with a state-of-the-art Fourier based method, the 'Eigenparticles' performs favorably showing clearly distinguishing the different particles.

Keywords Particle Characterisation; Particle Shape; Principle Components Analysis; Eigenparticles; Eigenfeatures; Eigenfaces

---

J.E. Higham, K. Benavides Meneses, A. Vaidheeswaran
National Energy Technology Laboratories,
US Department of Energy,
Collins Ferry Way,
Morgantown,
WV, USA E-mail: j.e.higham@liverpool.ac.uk

P. Shepley
Department of Civil and Structural Engineering,
University of Sheffield,
Mappin Street,
Sheffield, UK

1 Introduction

Characterization of a particle's morphology is the corner stone of many engineering applications. It is essential for an accurate description of solids used in the energy sector (Yi et al., 2008), pharmaceutical industries, food production (Wu, 2008; Markauskas et al., 2015), soil mechanics (Rousé et al., 2008; Shinohara et al., 2000) and countless other disciplines. With the advent and accessibility of high performance computing, the use of Discrete Element Modelling (DEM) approach (Cundall and Strack, 1979) based on Lagrangian formulation is steadily becoming common place for modelling such applications. In most cases, DEM implementation is consistent while modeling spherical particles.

In the past few years, several DEM approaches have been developed to consider non-spherical particles (Langston et al., 2004; Jin et al., 2011; Dong et al., 2015; Zhong et al., 2016). These utilize several existing mathematical techniques to describe non-spherical and irregular shapes which include super quadrics (Barr, 1981; Williams and Pentland, 1992), polygons and polyhedrons (Lee et al., 2009; Nassauer et al., 2013) or potential particles (Lee et al., 2009; Nassauer et al., 2013) (the reader is directed to Lu et al. (2015) for a full review). However obtaining the morphological information to describe these irregular non-spherical particles is non-trivial. Despite the known effects of particle shape on granular characteristics including friction angles (Nouguier-Lehon et al., 2003), hydraulic conductivity (Rousé et al., 2008; Shinohara et al., 2000), creep under constant effective stress (Leung et al., 1996; Oda, 1972) and small strain deformations (Santamarina and Cascante, 1998), there is a lack of significant body of work to describe non-spherical and irregular particles. Hence, it is common to use simplistic assumptions while modelling based on conventional measures such as sphericity or roundness (Krumbein, 1941; Rittenhouse, 1943). These have been proven to be inadequate for several practical applications such as hopper discharge (Cleary and Sawley, 2002), fluidized beds (Oschmann et al., 2014) and pneumatic conveying (Zhong et al., 2016). In order to create reliable predictions there is clearly a need for a comprehensive and efficient method to better describe the morphology of particles.

Previous attempts at quantitative characterization have been made using shape factors (Wadell, 1932; Heywood, 1954), fractal descriptors (Orford and Whalley, 1983; Vallejo, 1995; Hayward et al., 1989), Fourier descriptors (Clark, 1981; Kiryati and Maydan, 1989; Luerkens et al., 1982; Bowman et al., 2001), and more recently three-dimensional space filling (Nie et al., 2018). However, each of these methods rely on geometrical descriptions based on the definition of a material boundary and / or the composition of different shapes. A straightforward implementation of these methods for large-scale practical applications would be computationally inefficient.

In this study, we propose an alternative route for particle characterization based on the robust, algorithmic, facial recognition technique 'Eigenfaces' (Sirovich and Kirby, 1987; Turk and Pentland, 1991). We use this method to describe different particle geometrical features based on their degree of similarity to a set of basis shapes creating a similarity index. Whilst this index does not offer a high fidelity description that captures the particle's surface texture, it does generate a set of input values that describe the overall shape through a series of terms. This method could eventually be related to the existing shape generation approaches such as Barr (1981) and Williams and Pentland (1992). The work presented is organized as follows: First the Eigenface method is introduced and the mathematical implementation described. Next the method is applied to a set of synthetic data to demonstrate the methods applicability, before being applied to real distributions of two-dimensional images of segmented particles. Finally the work concludes by presenting some important observations on the proposed technique and proffers some ideas for its future implementation.

2 Eigenparticle method: Description

The Eigenface approach first proposed by Sirovich and Kirby (1987) & Turk and Pentland (1991) is a method based on a Principal Component Analysis (PCA) (Kosambi, 1943; Loève, 1945; Karhunen, 1946; Pougachev, 1953; Obukbov, 1954) developed to find similarities between sample images and low-order Eigen-representations of training image sets. The method is termed the 'Eigenface' method due to its popularity for facial recognition as by using training sets of human faces are used to create sets of 'Eigenfaces' it is used for facial recognition. This method is currently considered to be one of the most accurate and robust methods. The method is currently considered to be one of the most accurate and robust methods (Chellappa et al., 1995; Hsu et al., 2002; Tuzel et al., 2006). For a more detailed explanation regarding the Eigenfaces technique and the application to human faces, the reader is directed to the work of of Sirovich and Kirby (1987) & Turk and Pentland (1991).

In this study we extend the usage of the method to single particle analysis, coining the method the Eigenparticle method. As in the Eigenface method we provide a training set of images to create the 'Eigenparticles' to compare sample data against. However here instead of comparing distinctive facial features we use it to describe similarities in geometrical form. For this we create the training set from six basis shapes: A square, triangle, circle and their elongated forms respectively (see Fig. 2). Creating a set Eigenparticles from these basis shapes and comparing then to two-dimensional images of single particles we create a single number similarity index, to describe the similarities between the particle data and basis shapes. For the readers attention, the basis shapes we chose could be extended, different geometries or even real particle data could be used; we use these basic shapes merely to set foundation for future uses. The objective here is to propose and validate the idea of representing particles using Eigenparticles. Determining the optimum number of basis shapes requires a rigorous analysis and is beyond the scope of the work presented.

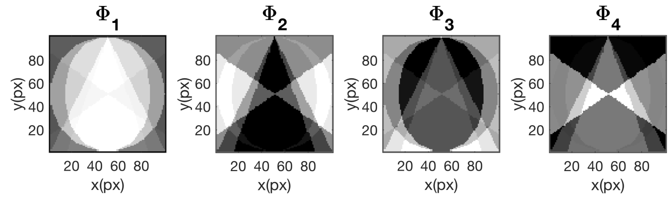

Fig. 1: Example of top four Eigenparticles used to create to form the comparison matrix of the basis shapes.

2.1 Creating the Eigenparticles

To determine the Eigenparticles ($\mathbf{F}$), which will be used to compare against the single particle data first we define a set of $n = 1, 2 \ldots \mathrm{N}$ binary basis shapes $\mathbf{I}_t(x, y; n)$ each with the same spatial $x = 1, 2, \ldots X$ and $y = 1, 2, \ldots Y$ dimensions. These two-dimensional basis shapes are then vector transformed and concatenated to form the matrix $\mathbf{I}(z, n)$ where $z = 1, 2, \ldots XY$ and the training matrix $\mathbf{I}_a(z, n)$ is formed by subtracting the spatial ensemble mean:

$$\mathbf{I}_a = \mathbf{I} - \sum_{n=1}^{N} \mathbf{I} \tag{1}$$

The comparison matrix ($\mathbf{F}$) is then created by multiplying a user defined number M of Eigenvectors (the Eigenparticles) determined via a PCA (where $m = 1, 2, \ldots M$):

$$\mathbf{F} = \boldsymbol{\Phi}(\mathbf{x}, \mathrm{M})^T \mathbf{I}_a, \tag{2}$$

where $\mathbf{F} \in \mathbb{R}^{\mathrm{M} \times \mathrm{N}}$. An example of these Eigenparticles ($\boldsymbol{\Phi}$) can be found in Fig. 1.

2.2 Comparing the particle data

When comparing the two-dimensional, binary particle data to the Eigenparticles there are two problems which need to be overcome; the Eigenparticle method is sensitive to both scale and to rotation. As real particle data have different sizes and the orientations often change we overcome these caveats by creating Θ=360 replicas of each particle, each rotionally transformed by $\theta = 1, 2, \ldots \Theta$ degrees about the centroid and scale them using a linear interpolate to have the same two-dimension dimensions as the training images, but not modifying the aspect ratio. From these data we create the matrix $\mathbf{P}_c(z, \theta)$ by again vector transforming and concatenating the images. By multiplying the same user defined number M of Eigenvectors and subtracting the ensemble mean of the training images we obtain the comparison matrix $\mathbf{G}$:

$$\mathbf{G} = \boldsymbol{\Phi}(x, \mathrm{M})^T (\mathbf{P}_c - \sum_{n=1}^{N} \mathbf{I}) \tag{3}$$

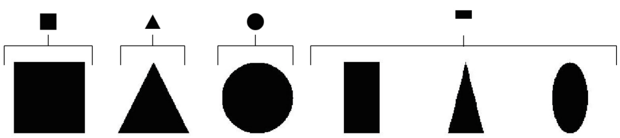

Fig. 2: Example of the training images used to compute the Eigenparticles, and bins used to describe the morphology of the particles. Where the square relates to the squareness (■), triangle relates to the triangularly (▲), circle relates to circularity (●) and rectangles related to the elongation (-).

where $\mathbf{G} \in \mathbb{R}^{\mathrm{M} \times \Theta}$. By minimizing each rotation to $\mathbf{F}$, it is possible to create a similarity index relating to each basis shape (n) for each rotation (θ):

$$\mathbf{W} = \underset{m \in \Theta}{\text{minimize}} ||\mathbf{F} - \mathbf{G}|| \tag{4}$$

where $\mathbf{W} \in \mathbb{R}^{\mathrm{N},\Theta}$ and $|| \cdot ||$ is the L_2 norm. These weights are viewed as similarity indices show how similar the sample particles are compared to the basis shapes for each direction. By finding the maximum value of each n from all θ's thus gives a measure of the optimum directional match for the basis images $W_{\max}$:

$$W_{\max} = \max_{n \in \Theta} \{\mathbf{W}\} \tag{5}$$

where $W_{\max} \in \mathbb{R}^{\mathrm{N}}$, and in this vector a value of 0 indicated no similarity ranging to 1 indicating a perfect similarity to the base images. Thus in this case giving a measure of squareness (■), triangularity (▲), circularity (●), and by averaging the results of their elongated forms, elongation (-) (see Fig. 2).

3 Eigenparticle method: Application

In this study we first apply the method to synthetic images of particles, before applying the method to samples of segmented binary images of single particles obtained from commercially available QICPIC (manufactured by Sympatec GmbH) at the U.S. Department of Energy's National Energy Technology Laboratory. QICPIC uses a light scattering method to analyse particles sized between 0.5 micron and 6.8 mm. A comprehensive granular material database characterized using QICPIC is made publicly available [1]. When the Eigenparticle method is applied, in both cases X = 100pixels, Y = 100pixels, M = 4 and N = 6 (see Fig. 2). For both cases we also compare the results to existing methods to highlight it's benefits. We compare the method to sphericity ($\mathrm{S_p}$), roundness ($\mathrm{R_p}$),b ased on the work of Krumbein (1941) & Rittenhouse (1943) and implemented as in Zheng and Hryciw (2015). We also compare our results to the state-of-the-art Fourier based method proposed by Bowman et al. (2001). Here the boundary co-ordinates are decomposed using a Fourier

[1] https://mfix.netl.doe.gov/experimentation/granular-materials-database/

transform and the Fourier coefficient used to describe Elongation (-1), Triangularity (-2), Squareness (-3) and Asymmetry (+1). For a full description of the method the reader is directed to (Bowman et al., 2001).

As with all processing based techniques the computational time, especially if large samples are uses, is extremely important. Of course due to the simplicity of the operations the sphericity and roundness factors out perform the Fourier and Eigenparticle methods where time is sacrificed for higher fidelity measurments. Between these two methods, at least in the experiments undertaken in the study, there is little time difference each method having their associated advantages and disadvantages. The computationally expensive part of the Fourier based method relates to the boundary detection and computation of the Fourier transform. The computationally expensive part of the Eigenparticle method relates to the 360 operations to minimize the comparisons. Although as none of the authors are computer scientists, and of course such factors are language and architecture dependent, it is not possible to create any definite statements.

3.1 Synthetic Data

As shown in Table. 1 eight idealised shapes are chosen. $S_p = 1$ for a perfectly spherical particle and it starts to deviate from 1 mainly in the presence of surface irregularities, blockiness in shape and elongation. Square (a) has a sphericity value of 0.91 higher than the irregular circle (f) which has a value of 0.84. This supports the argument that sphericity alone may not be sufficient to characterize non-spherical particles. For the square shape, the weight factors corresponding to circle, triangle and elongation are 0, while for the irregular circle, the weight factors corresponding to elongation alone is 0. There are minor contributions from square and triangle due to irregularities imposed on the circle. Similar observations could be made for roundness of different geometries. Rectangle (b) has a greater roundness compared to ellipse (d). Also, the roundness of triangle (e) is similar to ellipse (d). This suggests that roundness, like sphericity, by itself is inadequate to characterize the particles. In Table 1 the results of Bowman et al. (2001) are also presented. Here we do not go into to much detail as the shapes which are chosen the same geometries as used the Bowman et al. (2001) and almost identical results are obtained, with minor differences likely to be associated to the small differences in input images.

As presented in Table. 1 when the Eigenparticle technique is applied, significant differences emerge. Here quite clearly the method is able to make clear distinctions between the different shapes. As expected for (a-e), when similar shapes to the basis shapes are uses there are clear matched. However, for cases (f-h) where noise is added, quite clearly the Eigenparticles methods performs well at distinguishing the main underlying shape. Also interesting for (h) the method determines that the shape is fairly triangular (▲=0.83) but also has aspects circular features (•=0.23). Hence, instead of characterizing particles

	Particle	S_p	R_p	Fourier Coefficients	Eigenparticle
(a)		0.91	0.27	(-1) : 0.0000 (-2) : 0.0013 (-3) : 0.1230 (+1) : 0.0013	(■): 1.00 (▲) : 0.00 (•) : 0.00 (-) : 0.00
(b)		0.56	0.46	(-1) : 0.2480 (-2) : 0.0002 (-3) : 0.0745 (+1) : 0.0093	(■): 0.71 (▲) : 0.00 (•) : 0.00 (-) : 1.00
(c)	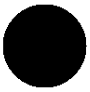	1.00	1.00	(-1) : 0.0000 (-2) : 0.0000 (-3) : 0.0000 (+1) : 0.0000	(■): 0.00 (▲) : 0.00 (•) : 1.00 (-) : 0.00
(d)		0.93	0.57	(-1) : 0.2447 (-2) : 0.0028 (-3) : 0.0278 (+1) : 0.0155	(■): 0.00 (▲): 0.00 (•) : 0.68 (-) : 1.00
(e)		0.79	0.52	(-1) : 0.2120 (-2) : 0.2412 (-3) : 0.0222 (+1) : 0.0139	(■): 1.00 (▲): 0.00 (•) : 0.00 (-) : 0.00
(f)	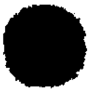	0.54	0.52	(-1) : 0.0011 (-2) : 0.0054 (-3) : 0.0233 (+1) : 0.0038	(■): 0.01 (▲): 0.08 (•) : 0.82 (-) : 0.00
(g)		0.54	0.21	(-1) : 0.0237 (-2) : 0.0725 (-3) : 0.1017 (+1) : 0.0744	(■): 0.86 (▲): 0.05 (•) : 0.00 (-) : 0.08
(h)		0.56	0.50	(-1) : 0.0284 (-2) : 0.2453 (-3) : 0.0061 (+1) : 0.0095	(■): 0.06 (▲): 0.83 (•) : 0.23 (-) : 0.02

Table 1: Idealised particle geometries used to highlight the method. S_p is the sphericity parameter, R_p is roundness parameter. The Fourier Coefficients are the same as those found in Bowman et al. (2001) where (-1) relates to elongation, (-2) squareness, (-3) triangularity and (+1) asymmetry. The Eigenparticles relate to the basis shapes defining the squareness (■), triangularity (▲), roundness (•) and elongation (-).

based on sphericity, roundness or Fourier coefficients basis shapes could be used efficiently to describing them. It must be noted that the basis shapes chosen in this study might not be the most ideal set to represent the features for different particles.

3.2 Application to particle data

In the section data created from a QICPIC is characterized. The data created by the QICPIC is binary segmented image data. In all 10 different types of material were selected (2mm Cones, Acrylic Diamonds, Angular Sand, Ceramic Pellets, Duralum 2, Glass Beads, NaCl, Nylon Cylinders, Sand Black, Sucrose Beads). Examples microscope images of each material can be found in Table **??** (these data are not used for any computations) and examples of the raw segmented binary images used in the calculations can be found on the bottom row of each sub-figure in Fig 3. It can be seen that the shapes are highly non-spherical and irregular. This reiterates the fact that using a sphericity or roundness factor would be inadequate to model such particles in a system. Again for all of these data the sphericity, roundness, Fourier coefficients and Eigenparticle similarity indexes are calculated. As there are many particles in each sample, we present the results in two manors. In Table **??** a statistical representation of the mean and standard deviation values for each sample of material is presented. In Figs 3(a-j) the histograms of these quantities are presented, and for reference some instantaneous results of all of the methods are presented on the bottom row.

From these data and the results presented in Table **??** & Figs 3(a-j) it seems the Fourier coefficients in most of the cases are unable to successfully elucidate the different geometrical features. On the other hand it seems that the Eigenparticle method achieves great some successes. The success of the method is particularly highlighted in the 2mm Cones where the method is able to identify the elongated triangularity and circularity and the Nylon cylinders where it is able to match the squareness and circularity. Hence, the Eigenparticle method offers an elegant approach to characterise non-spherical and irregular shapes. This information could offer the ever needed extra for reducing error modelling granular and multi-phase flow systems by using realistic particle shapes.

4 Conclusions

This work presents a novel particle characterization technique, i.e., the Eigenparticle method, based on the well utilised Eigenfaces facial recognition technique. Basis shapes are used to determine the extent of squareness, circularity, triangularity and elongation of a given particle. The results are presented in the form of a distribution with a statistical mean and standard deviation and the histograms of the raw data corresponding to the similarity indexes to prescribed basis shapes. This method provides more details regarding the morphology hidden in classical definitions of sphericity and roundness. Some of the shortcomings of using sphericity, roundness factors and Fourier coefficients methods are highlighted and resolved through the demonstrated ability of the Eigenparticle approach. The proposed technique is shown to be efficient and robust based on its ability to characterize a wide range of particles. The analysis using this method could offer to be extremely useful when providing morphological information to advance modelling capabilities.

Case	Material	S_p	R_p	Fourier Coefficients	EigenParticle
(a)	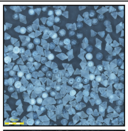	0.75 ± 0.14	0.37 ± 0.09	(-1) : 0.039 ± 0.037 (-2) : 0.052 ± 0.047 (-3) : 0.017 ± 0.017 (+1) : 0.044 ± 0.040	(■): 0.155 ± 0.101 (▲): 0.308 ± 0.262 (●) : 0.310 ± 0.326 (-) : 0.294 ± 0.190
(b)	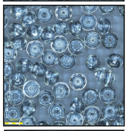	0.92 ± 0.14	0.35 ± 0.10	(-1) : 0.045 ± 0.039 (-2) : 0.020 ± 0.020 (-3) : 0.012 ± 0.011 (+1) : 0.076 ± 0.050	(■): 0.030 ± 0.025 (▲): 0.018 ± 0.018 (●) : 0.469 ± 0.466 (-) : 0.393 ± 0.374
(c)	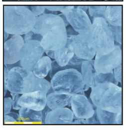	0.82 ± 0.13	0.47 ± 0.09	(-1) : 0.142 ± 0.092 (-2) : 0.057 ± 0.050 (-3) : 0.031 ± 0.026 (+1) : 0.158 ± 0.087	(■): 0.084 ± 0.078 (▲): 0.183 ± 0.160 (●) : 0.227 ± 0.237 (-) : 0.437 ± 0.189
(d)	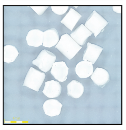	0.90 ± 0.10	0.33 ± 0.08	(-1) : 0.040 ± 0.037 (-2) : 0.017 ± 0.014 (-3) : 0.026 ± 0.022 (+1) : 0.048 ± 0.037	(■): 0.113 ± 0.153 (▲): 0.049 ± 0.044 (●) : 0.498 ± 0.298 (-) : 0.332 ± 0.307
(e)	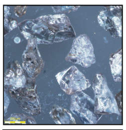	0.91 ± 0.11	0.41 ± 0.11	(-1) : 0.046 ± 0.055 (-2) : 0.019 ± 0.021 (-3) : 0.012 ± 0.013 (+1) : 0.053 ± 0.060	(■): 0.056 ± 0.050 (▲): 0.048 ± 0.061 (●) : 0.661 ± 0.340 (-) : 0.230 ± 0.279
(f)	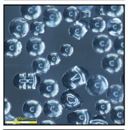	0.97 ± 0.06	0.47 ± 0.09	(-1) : 0.014 ± 0.030 (-2) : 0.007 ± 0.012 (-3) : 0.006 ± 0.007 (+1) : 0.017 ± 0.036	(■): 0.033 ± 0.031 (▲): 0.018 ± 0.035 (●) : 0.888 ± 0.193 (-) : 0.070 ± 0.154
(g)	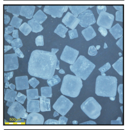	0.92 ± 0.10	0.34 ± 0.10	(-1) : 0.041 ± 0.041 (-2) : 0.016 ± 0.017 (-3) : 0.025 ± 0.019 (+1) : 0.046 ± 0.050	(■): 0.089 ± 0.077 (▲): 0.050 ± 0.045 (●) : 0.639 ± 0.273 (-) : 0.226 ± 0.258
(h)	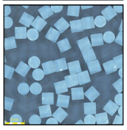	0.92 ± 0.10	0.32 ± 0.06	(-1) : 0.039 ± 0.032 (-2) : 0.010 ± 0.012 (-3) : 0.030 ± 0.026 (+1) : 0.051 ± 0.034	(■): 0.325 ± 0.279 (▲): 0.035 ± 0.030 (●) : 0.588 ± 0.250 (-) : 0.077 ± 0.084
(i)	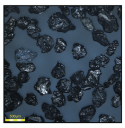	0.81 ± 0.13	0.34 ± 0.07	(-1) : 0.085 ± 0.063 (-2) : 0.039 ± 0.030 (-3) : 0.024 ± 0.019 (+1) : 0.103 ± 0.069	(■): 0.055 ± 0.057 (▲): 0.093 ± 0.083 (●) : 0.238 ± 0.260 (-) : 0.529 ± 0.236
(j)	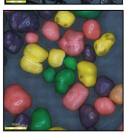	0.88 ± 0.13	0.35 ± 0.09	(-1) : 0.049 ± 0.043 (-2) : 0.021 ± 0.017 (-3) : 0.012 ± 0.010 (+1) : 0.063 ± 0.045	(■): 0.067 ± 0.064 (▲): 0.056 ± 0.050 (●) : 0.470 ± 0.339 (-) : 0.404 ± 0.337

Table 2: Statistical results for different particle materials and number of particles sampled (a) 2mm Cones - 351 (b) Acrylic Diamonds - 59 (c) Angular Sand - 1570 (d) Ceramic Pellets - 1660 (e) Duralum 2 - 10507 (f) Glass Beads - 10756 (g) NaCl - 10406 (h) Nylon Cylinders - 1049 (i) Sand Black -10413 (j) Sucrose Beads - 1508. First column shows example photograph of each material (not used in any calculations). Second and third column shows the average and standard deviations or the sphericity and roundness. Fourth column show the average and standard deviations of the Fourier Coefficient as found in Bowman et al. (2001) where (-1) relates to elongation, (-2) squareness, (-3) triangularity and (+1) asymmetry. Fifth column shows the average and standard deviations of the Eigenparticles relating to the basis shapes defining the squareness (■), triangularity (▲), roundness (●) and elongation (-).

5 Acknowledgements

The first author funding provided by Oakridge Institute for Science and Education. Second author with funding in part through the Engineering and Physical Sciences Research Council, UK (Grant Number R/147129).

6 Ethical Statement

This submission is fully compliant with the Ethical Standards of the journal. This work is a novel study not presented or published by these authors' previously.

References

Barr AH (1981) Superquadrics and angle-preserving transformations. IEEE Computer graphics and Applications 1(1):11–23

Bowman ET, Soga K, Drummond W (2001) Particle shape characterisation using fourier descriptor analysis. Geotechnique 51(6):545–554

Chellappa R, Wilson CL, Sirohey S (1995) Human and machine recognition of faces: A survey. Proceedings of the IEEE 83(5):705–741

Clark MW (1981) Quantitative shape analysis: a review. Journal of the International Association for Mathematical Geology 13(4):303–320

Cleary PW, Sawley ML (2002) Dem modelling of industrial granular flows: 3d case studies and the effect of particle shape on hopper discharge. Applied Mathematical Modelling 26(2):89–111

Cundall PA, Strack OD (1979) A discrete numerical model for granular assemblies. geotechnique 29(1):47–65

Dong K, Wang C, Yu A (2015) A novel method based on orientation discretization for discrete element modeling of non-spherical particles. Chemical Engineering Science 126:500–516

Hayward J, Orford JD, Whalley WB (1989) Three implementations of fractal analysis of particle outlines. Computers & Geosciences 15(2):199–207

Heywood H (1954) Particle shape coefficitnts. J Imperial College Chemical Society 8:25–33

Hsu RL, Abdel-Mottaleb M, Jain AK (2002) Face detection in color images. IEEE transactions on pattern analysis and machine intelligence 24(5):696–706

Jin F, Xin H, Zhang C, Sun Q (2011) Probability-based contact algorithm for non-spherical particles in dem. Powder technology 212(1):134–144

Karhunen K (1946) Zur spektral theorie stochastischer prozesse. Annales Academiæ Scientiarum Fennicæ A1:34

Kiryati N, Maydan D (1989) Calculating geometric properties from fourier representation. Pattern Recognition 22(5):469–475

Kosambi D (1943) Statistics in function space. Journal of Indian Mathematical Society 7:76–88

Krumbein WC (1941) Measurement and geological significance of shape and roundness of sedimentary particles. Journal of Sedimentary Research 11(2):64–72

Langston PA, Al-Awamleh MA, Fraige FY, Asmar BN (2004) Distinct element modelling of non-spherical frictionless particle flow. Chemical Engineering Science 59(2):425–435

Lee J, Ghosh K, Stang PJ (2009) Stoichiometric control of multiple different tectons in coordination-driven self-assembly: Preparation of fused metallacyclic polygons. Journal of the American Chemical Society 131(34):12028–12029

Leung C, Lee F, NS Y (1996) The role of particle breakage in pile creep in sand. Canadian Geotechnical Journal 33(6):888–898

Loève M (1945) Functions aleatoire de second ordre. Comptes Rendus de l'Académie des Sciences 220

Lu G, Third J, Müller C (2015) Discrete element models for non-spherical particle systems: from theoretical developments to applications. Chemical Engineering Science 127:425–465

Luerkens DW, Beddow JK, Vetter A (1982) Morphological fourier descriptors. Powder Technology 31(2):209–215

Markauskas D, Ramírez-Gómez Á, Kačianauskas R, Zdancevičius E (2015) Maize grain shape approaches for dem modelling. Computers and Electronics in Agriculture 118:247–258

Nassauer B, Liedke T, Kuna M (2013) Polyhedral particles for the discrete element method. Granular Matter 15(1):85–93

Nie Z, Liang Z, Wang X (2018) A three-dimensional particle roundness evaluation method. Granular Matter 20(2):32

Nouguier-Lehon C, Cambou B, Vincens E (2003) Influence of particle shape and angularity on the behaviour of granular materials: a numerical analysis. International Journal for Numerical and Analytical Methods in Geomechanics 27(14):1207–1226

Obukbov AM (1954) Statistical description of continuous fields. Trudy Geofizicheskogo Instituta, Akademiya Nauk SSSR 24:3–42

Oda M (1972) Initial fabrics and their relations to mechanical properties of granular material. Powder Technology 12(1):17–36

Orford J, Whalley W (1983) The use of the fractal dimension to quantify the morphology of irregular-shaped particles. Sedimentology 30(5):655–668

Oschmann T, Hold J, Kruggel-Emden H (2014) Numerical investigation of mixing and orientation of non-spherical particles in a model type fluidized bed. Powder Technology 258:304–323

Pougachev VS (1953) General theory of the correlations of random functions. Izvestiya Akademii Nauk SSSR Seriya Matematicheskaya Bulletin de l'Académie des Sciences de l'URSS

Rittenhouse G (1943) A visual method of estimating two-dimensional sphericity. Journal of Sedimentary Research 13(2)

Rousé P, Fannin R, Shuttle D (2008) Influence of roundness on the void ratio and strength of uniform sand. Géotechnique 58(3):227–231

Santamarina C, Cascante G (1998) Effect of surface roughness on wave propagation parameters. Géotechnique 48(1):129–136

Shinohara K, Oida M, Golman B (2000) Effect of particle shape on the angle of internal friction by triaxial compression test. Powder Technology 107(1):131–136

Sirovich L, Kirby M (1987) Low-dimensional procedure for the characterization of human faces. Josa a 4(3):519–524

Turk M, Pentland A (1991) Eigenfaces for recognition. Journal of cognitive neuroscience 3(1):71–86

Tuzel O, Porikli F, Meer P (2006) Region covariance: A fast descriptor for detection and classification. In: European conference on computer vision, Springer, pp 589–600

Vallejo LE (1995) Fractal analysis of granular materials. In: International Journal of Rock Mechanics and Mining Sciences and Geomechanics Abstracts, vol 8, p 371A

Wadell H (1932) Volume, shape and roundness of rock particles. Journal of Geology 40(5):443–451

Williams JR, Pentland AP (1992) Superquadrics and modal dynamics for discrete elements in interactive design. Engineering Computations 9(2):115–127

Wu CY (2008) Dem simulations of die filling during pharmaceutical tabletting. Particuology 6(6):412–418

Yi H, Hao J, Duan L, Tang X, Ning P, Li X (2008) Fine particle and trace element emissions from an anthracite coal-fired power plant equipped with a bag-house in china. Fuel 87(10-11):2050–2057

Zheng J, Hryciw R (2015) Traditional soil particle sphericity, roundness and surface roughness by computational geometry. Géotechnique 65(6):494–506

Zhong W, Yu A, Liu X, Tong Z, Zhang H (2016) Dem/cfd-dem modelling of non-spherical particulate systems: theoretical developments and applications. Powder Technology 302:108–152

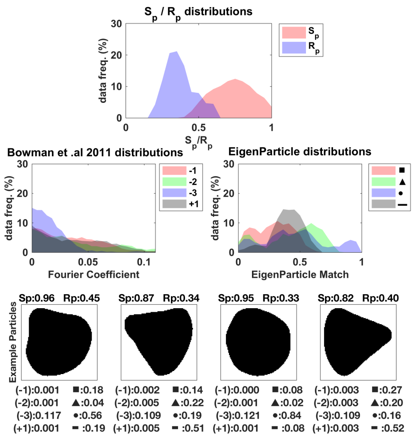

(a) 2mm Cones

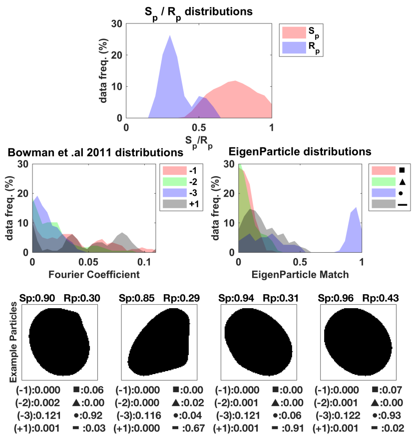

(b) Acrylic Diamonds

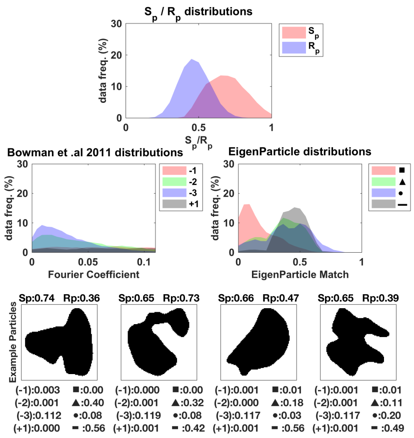

(c) Angular Sand

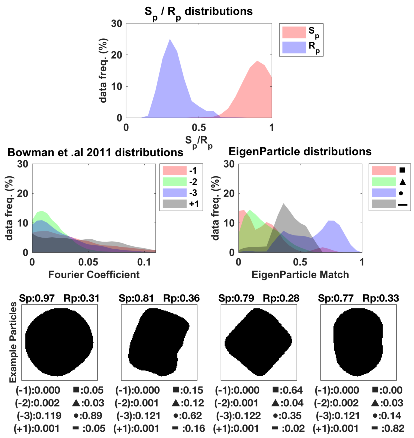

(d) Ceramic Pellets

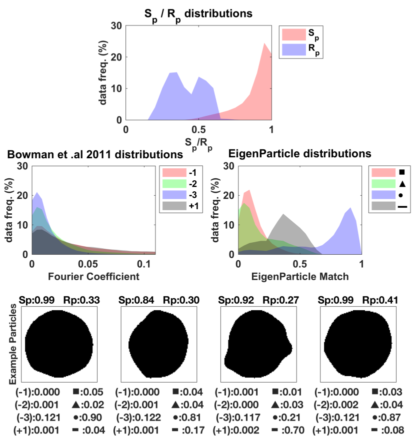

(e) Duralum 2

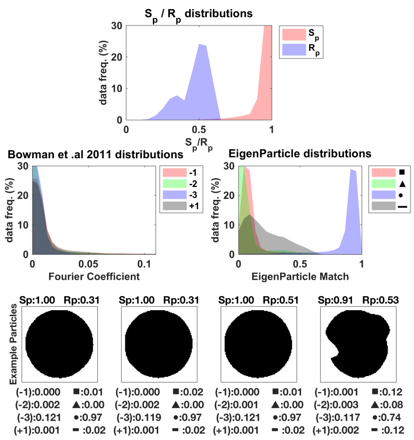

(f) Glass Beads

Fig. 3: Raw results for different particle materials and number of particles sampled (a) 2mm Cones - 351 (b) Acrylic Diamonds - 59 (c) Angular Sand - 1570 (d) Ceramic Pellets - 1660 (e) Duralum 2 - 10507 (f) Glass Beads - 10756 (g) NaCl - 10406 (h) Nylon Cylinders - 1049 (i) Sand Black -10413 (j) Sucrose Beads - 1508. Top row shows histogram of Sphericity (S_p) and Roundness (R_p). Middle row show left shows Fourier Coefficient histograms, right shows Eigenparicle similarity index histograms. Bottom row shows examples of particle data with relative S_p and R_p, and Fourier Coeffients and Eigenparticle similarity indexes below

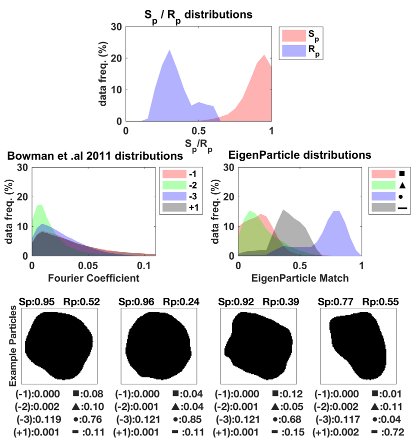

(g) NaCl

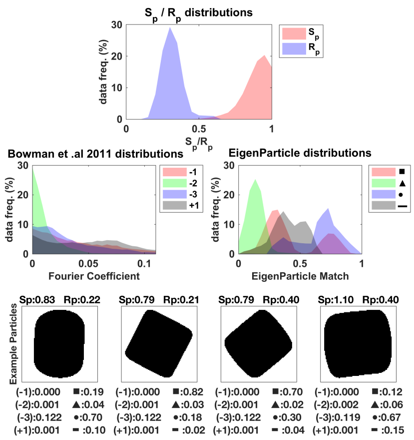

(h) Nylon Cylinders

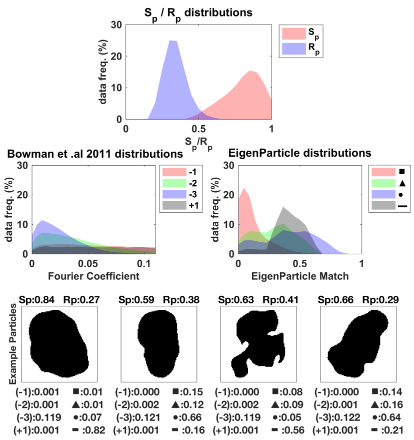

(i) Black Sand

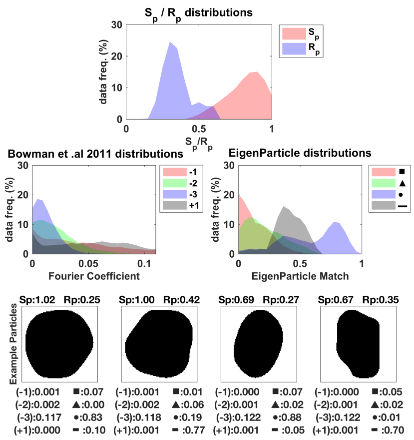

(j) Sucrose Beads

Fig. 3: cont.